PCCP

Photophysical properties and photocatalytic activities under visible light irradiation of silver vanadates

Ryoko Konta,[a] Hideki Kato,[a] Hisayoshi Kobayashi[b] and Akihiko Kudo*[ac]

[a] *Department of Applied Chemistry, Faculty of Science, Science University of Tokyo, 1-3 Kagurazaka, Shinjyuku-ku, Tokyo 162-8601, Japan. E-mail: a-kudo@rs.kagu.tus.ac.jp; Fax: +81-33235-2214*

[b] *Department of Chemistry and Bioscience, Kurashiki University of Science and the Arts, Nishinoura 2640, Tsurajima, Kurashiki, Okayama 712-8505, Japan*

[c] *Core Research for Evolutional Science and Technology, Japan Science and Technology Corporation (CREST, JST), 4-1-8 Honcho, Kawaguchi-shi, Saitama 332-0012, Japan*

Received 7th January 2003, Accepted 23rd May 2003
First published as an Advance Article on the web 12th June 2003

α-$AgVO_3$, β-$AgVO_3$, $Ag_4V_2O_7$ and Ag_3VO_4 prepared by precipitation and solid-state reactions showed intense absorption bands in the visible light region due to band gap transitions. Comparison of a diffuse reflectance spectrum of α-$NaVO_3$ with that of α-$AgVO_3$ with a diopside-type structure revealed that a band gap (2.5 eV) of α-$AgVO_3$ was 0.6 eV smaller than that (3.1 eV) of α-$NaVO_3$. The electronic band structure study using a plane-wave based density functional method indicated that the decrease in the band gap of α-$AgVO_3$ was due to Ag 4d orbitals which formed a valence band at a more negative level than O 2p orbitals. Among α-$AgVO_3$, β-$AgVO_3$, $Ag_4V_2O_7$ and Ag_3VO_4, only Ag_3VO_4 showed a photocatalytic activity for O_2 evolution from an aqueous silver nitrate solution under visible light irradiation. Holes photogenerated in Ag_3VO_4 can migrate to the reaction sites on the surface more easily than those of other silver vanadates, because the content of silver forming a valence band is large. It resulted in that holes photogenerated in Ag_3VO_4 are able to oxidize H_2O to form O_2.

Introduction

The photocatalytic water splitting into H_2 and O_2 which is an ideal way to get H_2 from water has extensively been studied. Various oxide photocatalysts which are able to decompose water efficiently have been reported up to now.[1–3] However, most of them do not respond to visible light, because they have wide band gaps (BG $>$ 3 eV). Although a new photocatalyst, $In_{0.9}Ni_{0.1}TaO_4$, which is able to split water into H_2 and O_2 in stoichiometric amounts under visible light irradiation has recently been reported by Zou, Arakawa and co-workers, the quantum yield is low and an available visible light region is thus limited.[4] Thus the development of photocatalysts efficiently working under visible light irradiation is still an important theme. As valence bands of oxide photocatalysts consisting of metal cations with d^0 and d^{10} configuration are usually composed of O 2p orbitals, the levels are usually deep (*ca.* 3 eV) compared with an oxidation potential of water to form O_2 ($E^0(O_2/H_2O) = 1.23$ V).[5] Therefore, it is indispensable that the valence band is formed at a more negative potential than the band composed of O 2p orbitals. There are some ways to design photocatalysts which absorb visible light. These include doping of a metal ion into a photocatalyst having a wide band gap (>3 eV),[6] through hybridization of N 2p and O 2p orbitals,[7] and formation of a valence band by other elements than oxygen.[8,9] The present authors have recently reported that $BiVO_4$ and $AgNbO_3$ can produce O_2 from an aqueous silver nitrate solution under visible light irradiation.[8,9] The visible light responses of the $BiVO_4$ and $AgNbO_3$ photocatalysts are attributable to a decrease in band gaps by the valence band formation by not only O 2p but also Bi 6s and Ag 4d orbitals.[8,9] The valence band of $AgTaO_3$, which is an active photocatalyst for water splitting under UV irradiation, also consists of O 2p and Ag 4d.[9] Therefore, it is interesting to survey silver compounds as candidates for visible light-driven photocatalysts. These visible light driven photocatalysts can evolve only H_2 and/or O_2 from aqueous solutions containing sacrificial reagents. However some of them may be used as a H_2 or O_2 evolution photocatalyst for construction of a Z-scheme system.[10]

In the present paper, we have paid attention to the control of the band structure by Ag^+ ions. Band structures and photocatalytic activities of oxides composed of silver and vanadium belonging to the same fifth group as tantalum and niobium are studied.

Experimental

Silver vanadate powders (α-$AgVO_3$, β-$AgVO_3$, $Ag_4V_2O_7$ and Ag_3VO_4) were prepared by solid-state and precipitation reactions. In the solid-state reaction, starting materials, Ag_2O (Kanto: 99.0%) and V_2O_5 (Wako: 99.0%), were mixed in a stoichiometric ratio and the mixtures were calcined at 640–670 K for 4–5 h in air using porcelain crucibles.[11–13] In the precipitation reaction, after the precipitate was produced by pouring an aqueous $AgNO_3$ (Tanaka Kikinzoku: 99.82%) solution into an aqueous NH_4VO_3 (Kanto: 99.0%) or Na_3VO_4 (Wako: 75.0%) solution, the mixed solutions were aged at 300 K for 1 day. Silver vanadates with different compositions were prepared by controlling pH and temperature.[11,12] The silver vanadate precipitate was washed with water, filtered, and dried at 320 K for 3–4 h. α-$NaVO_3$ was prepared by evaporating water from a mixed NH_4VO_3 (Kanto: 99.0%) and NaOH

(Kanto: 97.0%) solution on a hot plate.[13] The obtained powders were confirmed by X-ray diffraction (Rigaku; RINT-1400, MiniFlex). A Pt cocatalyst was loaded by a photoreduction method using an aqueous solution of $H_2PtCl_6{\cdot}6H_2O$ (Tanaka Kikinzoku: 37.55% as Pt).

Photocatalytic O_2 evolution from an aqueous silver nitrate solution and H_2 evolution from an aqueous methanol solution were carried out in a closed gas circulation system. The catalyst powder (0.3 g) was dispersed by a magnetic stirrer in a reactant solution (0.05 mol L^{-1} $AgNO_3$ aq. or 10 vol% MeOH aq., 150 mL) in the cell with a top window made of Pyrex. The light source was a 300 W Xe lamp (ILC technology: CERMAX LX-300F). Cut-off filters (HOYA) were employed for controlling wavelengths of irradiated light. Amounts of evolved gases were determined using a gas chromatography (Shimazu: GC-8A, MS-5A, TCD, Ar carrier).

Diffuse reflection spectra were obtained using UV-vis-NIR spectrometer (Jasco: UbestV-570) and were converted from reflection to absorbance by the Kubelka–Munk method. Photocatalyst powders were observed by a scanning electron microscope (Hitachi: S-5000). The specific surface areas of the samples were measured by the conventional Brunauer–Emmett–Teller (BET) method (Coulter, SA3100).

The plane wave based density functional method was carried out for α-$NaVO_3$ and α-$AgVO_3$ employing the CASTEP program.[14] The core electrons were replaced with the ultra-soft core potentials, and the valence electronic configurations for Na, V, Ag and O atoms were $2s^22p^63s^1$, $3s^23p^63d^34s^2$, $4d^{10}$-$5s^15p^0$ and $2s^22p^4$, respectively. The calculations were carried out using the primitive unit cells of $[\alpha\text{-}NaVO_3]_4$ and $[\alpha\text{-}AgVO_3]_4$, and the number of occupied orbitals were 80 and 84, respectively.

Results and discussion

Preparation of powders

Fig. 1 shows XRD patterns of silver vanadate powders prepared by precipitation and solid-state reactions. In the solid-state reaction, silver vanadate powders with different compositions were obtained by calcining staring materials mixed at stoichmetric ratios.[11–13] In the precipitation reaction, α-$AgVO_3$, β-$AgVO_3$, $Ag_4V_2O_7$ and Ag_3VO_4 were obtained by keeping the pH and the temperature of the reactant solutions at 7 and 273 K, 7 and 298 K, 11 and 298 K, and 14 and 298 K, respectively.[11,12] Half band widths of XRD patterns of silver vanadate powders prepared by the aqueous process, except α-$AgVO_3$, were almost the same as those prepared by solid-state reactions. This result indicates that well-crystallized silver vanadates were also able to be prepared in the aqueous process.

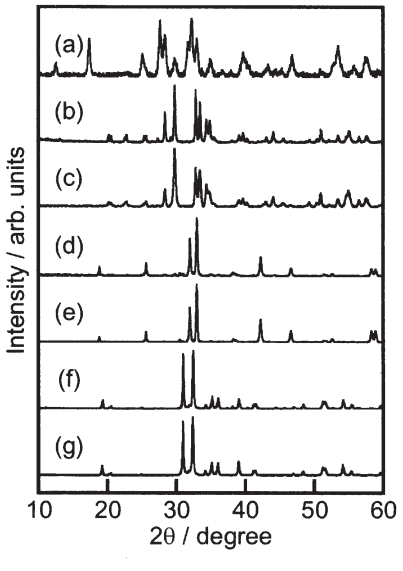

Fig. 1 X-Ray diffraction patterns of silver vanadates: (a) α-$AgVO_3$[2], (b) β-$AgVO_3$[1], (c) β-$AgVO_3$[2], (d) $Ag_4V_2O_7$[1], (e) $Ag_4V_2O_7$[2], (f) Ag_3VO_4[1] and (g) Ag_3VO_4[2]; [1] solid-state reaction, [2] precipitation reaction.

Contribution of Ag^+ to a valence band formation for α-$AgVO_3$

Diffuse reflectance spectra of α-$NaVO_3$ and α-$AgVO_3$ with a diopside-type structure are shown in Fig. 2.[11,15] The absorption edge of α-$NaVO_3$ was in the ultraviolet light region, while α-$AgVO_3$ possessed an intense absorption band in the visible light region. The band gaps of α-$NaVO_3$ and α-$AgVO_3$ estimated from the onsets of absorption edges were 3.1 eV and 2.5 eV, respectively. The band gaps of $AgTaO_3$ and $AgNbO_3$ in which valence bands consisted of Ag 4d and O 2p were 0.6 eV smaller than those of $NaTaO_3$ and $NaNbO_3$.[9] It was revealed that the band gap of α-$AgVO_3$ was also 0.6 eV smaller than that of α-$NaVO_3$ by substituting Ag^+ for Na^+ as observed in the cases of $AgTaO_3$ and $AgNbO_3$. The electronic structure of α-$NaVO_3$ and α-$AgVO_3$ were studied by a plane-wave based density functional method[14] in order to investigate how Ag^+ acted to decrease the band gap. Fig. 3 shows band structures and the density of state (DOS) of α-$NaVO_3$ and α-$AgVO_3$ while Fig. 4 shows density contour maps for LUMOs and HOMOs of α-$NaVO_3$ and α-$AgVO_3$. Six occupied bands and one unoccupied band in α-$NaVO_3$ and five occupied bands and one unoccupied band in α-$AgVO_3$ are shown in the DOS diagram in Fig. 3. The occupied orbitals of α-$NaVO_3$ were composed of V 3s, Na 2s, V 3p, Na 2p, O 2s and O 2p orbitals from the low energy side. The highest occupied orbital (*i.e.*, the top of valence band) consisted of only O 2p orbitals. The occupied orbitals of α-$AgVO_3$ were composed of V 3s, V 3p, O 2s, O 2p and Ag 4d orbitals from the low energy side. The occupied orbital at the highest energy orbital consisted of O 2p and Ag 4d orbitals. The lowest unoccupied orbital (*i.e.*, the bottom of conduction band) was mainly formed by V 3d orbitals in both α-$NaVO_3$ and α-$AgVO_3$. The calculated band gap (2.00 eV) of α-$AgVO_3$ was smaller than that (3.25 eV) of α-$NaVO_3$. Band gaps calculated by the present method are usually smaller than real band gaps. Closer agreement with experimental spectra requires the electron repulsion term as well as the one electron energy difference. This repulsion term works to reduce the transition energy, but is usually small for the transition between extended Bloch orbitals. Since the valence band of $NaVO_3$ is localized on the O 2p orbitals compared to that of α-$AgVO_3$, inclusion of the electron repulsion term may be more significant, and will recover the general trend of the underestimation of band gap. In α-$AgVO_3$, Ag 4d orbitals were involved in a formation of the top of the valence band (HOMO), but were not of the bottom of

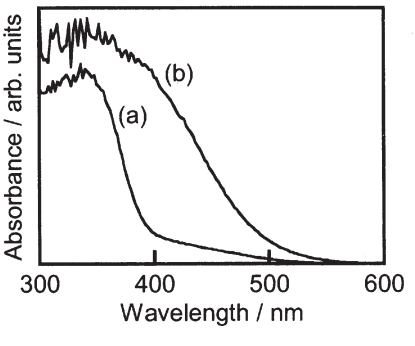

Fig. 2 Diffuse reflectance spectra of (a) α-$NaVO_3$ and (b) α-$AgVO_3$.

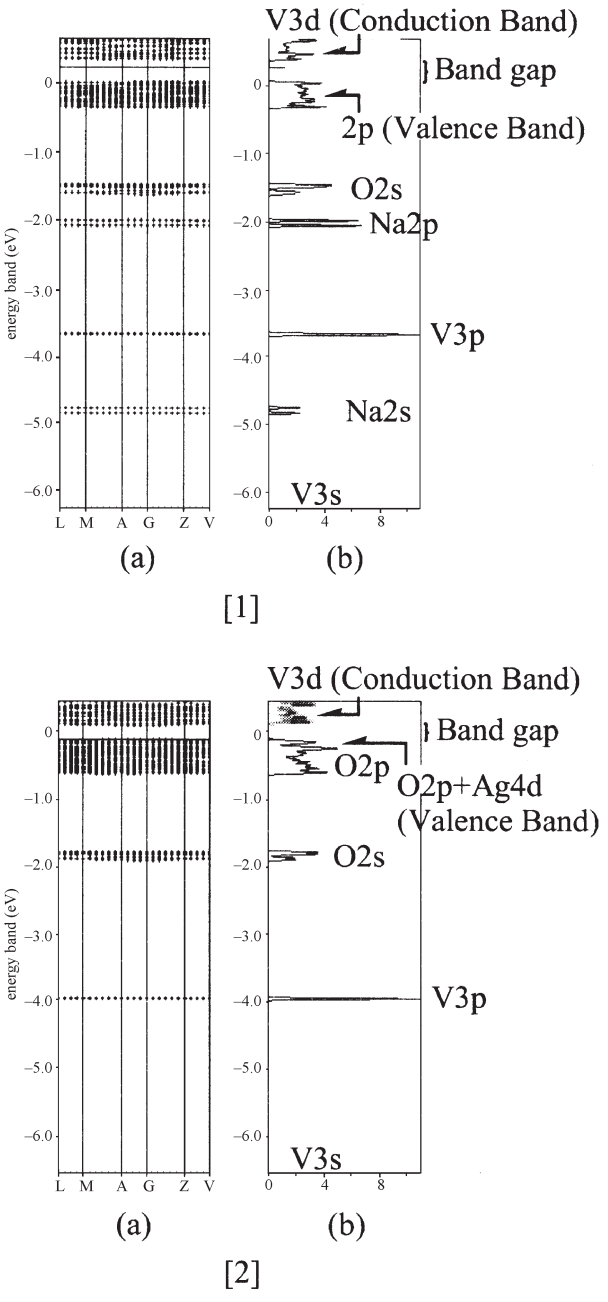

Fig. 3 Band structure and total density of state for α-$NaVO_3$ [1] and α-$AgVO_3$ [2] calculated by the density functional method.

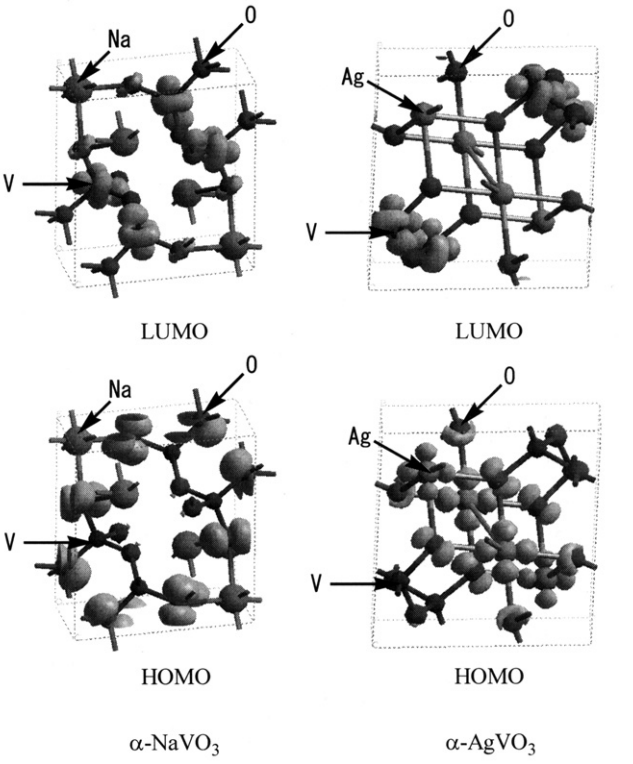

Fig. 4 Density contour maps for the LUMO and HOMO of α-$NaVO_3$ and α-$AgVO_3$ calculated by the density functional method.

conduction band (LUMO) as shown in Fig. 4. The valence bands of the metal oxides with d^0 metal cations as a constituent element, such as α-$NaVO_3$, are generally composed of O 2p orbitals, as clearly shown in Fig. 4. It was clarified by the theoretical calculation that Ag 4d orbitals formed a valence band with O 2p orbitals at the more negative level than native O 2p orbitals, resulting in the decrease in the band gap by substituting Ag for Na in α-$NaVO_3$ as shown in Fig. 2. It is reasonable for Ag^+ ions to have such an influence, judging from the redox potential (1.98 V *vs.* NHE) of Ag^{2+}/Ag^+ (although this refers to aqueous solution). This result provides important information to design new visible-light-driven photocatalysts.

Photophysical properties of silver vanadates

Fig. 5 shows diffuse reflectance spectra of four silver vanadate powders prepared by precipitation reactions. All the powders showed an intense absorption band in the visible light region ($\lambda > 420$ nm). In α-$AgVO_3$, $Ag_4V_2O_7$ and Ag_3VO_4, consisting of VO_4 tetrahedra, the onset of absorption shifted to longer wavelength as a ratio of silver to vanadium was increased. Band gaps of α-$AgVO_3$, $Ag_4V_2O_7$ and Ag_3VO_4 were estimated to be 2.5, 2.4 and 2.2 eV, respectively. As the ratio of silver was increased, the contribution of silver to the valence band formation became larger. It results in the decrease in the band gap accompanied with a negative potential shift of a valence band. On the other hand, the number of oxygen anions coordinating to a vanadium cation in α-type $AgVO_3$ is four while that of β-type is five. The smaller the coordination number of polyhedra of vanadates, the larger the interaction between a vanadium cation and oxygen anions, and the average bond length between V and O in four coordination is shorter than that in five coordination.[11,16] It also results in an increase in the energy gap between the HOMO and LUMO consisting of O 2p and V 3d orbitals, respectively. The change in the energy gap can also apply to the $AgVO_3$ in which the HOMO consists of Ag 4d and O 2p. Therefore, the band gap of α-type $AgVO_3$ is larger than that of β-type $AgVO_3$ in spite of the same composition.

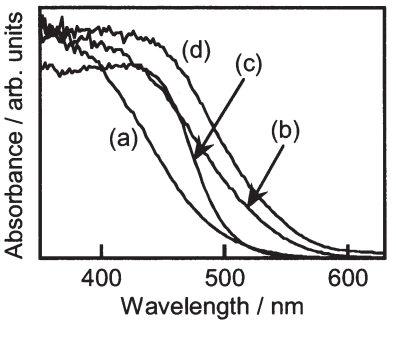

Fig. 5 Diffuse reflectance spectra of (a) α-$AgVO_3$, (b) β-$AgVO_3$, (c) $Ag_4V_2O_7$ and (d) Ag_3VO_4 prepared by precipitation reactions.

Photocatalytic activities of silver vanadates

The conduction band levels of silver vanadate photocatalysts used in the present work are not sufficient for H_2 evolution by reduction of water. Therefore, O_2 evolution from an aqueous silver nitrate solution was carried out as a photocatalytic test reaction. This reaction has often been used as a test reaction to investigate if a photocatalyst can generate O_2 by oxidation of water.[1] This reaction employs silver ions ($E^0(Ag^+/Ag) = 0.80$ V) as an electron scavenger. In this reaction, metallic silver is deposited on the catalyst surface, instead of H_2 evolution, by the reaction of silver ions with photogenerated electrons.

Table 1 shows O_2 evolution from an aqueous silver nitrate solution on silver vanadates under visible light irradiation ($\lambda > 420$ nm). Only Ag_3VO_4, which contained the highest amounts of silver and possessed the narrowest band gap among the tested silver vanadates, showed the O_2 evolution activity. In Ag_3VO_4, the photogenerated holes can easily migrate, and the reaction sites for O_2 evolution, which require four-electron oxidation of water are readily created on the surface, because the ratio of Ag^+ ions contributing to the valence band formation is large. These factors made Ag_3VO_4 powder active for the O_2 evolution.

X-Ray diffraction patterns of silver vanadates after the photocatalytic reaction were almost the same as those before the reaction, except for the existence of peaks due to photodeposited metallic silver. If vanadates were dissolved in water, the color of the solution should be yellow. However, the supernatants before and after the photocatalytic reaction were colorless. Moreover, even if Cl^- was added to the supernatant, a white precipitate of AgCl was not obtained. These results indicate that the elution and photocorrosion of silver vanadate are negligible.

The activity for O_2 evolution of Ag_3VO_4 photocatalysts prepared by a solid-state reaction was higher than that for photocatalysts prepared by a precipitation reaction. Ag_3VO_4 calcinated at 653 K for 4 h showed the highest activity for O_2 evolution from an aqueous silver nitrate solution under visible light irradiation. Scanning electron microscope measurements were carried out in order to attempt to rationalize the difference in the photocatalytic activity (Fig. 6). The particle size of Ag_3VO_4 prepared by precipitation reaction was smaller than that prepared by a solid-state reaction. However, sintered primary particles, in which a lot of grain boundaries should exist, were observed. In contrast, Ag_3VO_4 powders prepared by a solid-state reaction were well-crystallized. The BET surface areas of Ag_3VO_4 powder prepared by solid-state reaction and precipitation reaction were 0.2 and 2.7 $m^2\ g^{-1}$, respectively. This indicates that the difference in the photocatalytic activity between the preparation methods was not due to the surface area.

Table 1 Photocatalytic O_2 evolution from $AgNO_3$ aq. over silver vanadates prepared under different conditions

Catalyst	Preparation method	Preparation conditions	Activity/ μmol h^{-1}
α-$AgVO_3$	[2]	pH 7, 278 K	0
β-$AgVO_3$	[2]	pH 7, 298 K	0
β-$AgVO_3$	[1]	653 K, 4 h	0.6
$Ag_4V_2O_7$	[2]	pH 10–12, 298 K	0
$Ag_4V_2O_7$	[1]	633 K, 5 h	0.7
Ag_3VO_4	[2]	pH 14, 298 K	8
Ag_3VO_4	[1]	653 K, 4 h	17

Catalyst: 0.3 g, reactant solution: aqueous silver nitrate solution (0.05 mol L^{-1}, 150 mL), light source: 300 W Xe lamp with a cut-off filter ($\lambda > 420$ nm), cell: top irradiation type; [1] solid-state reaction, [2] precipitation reaction.

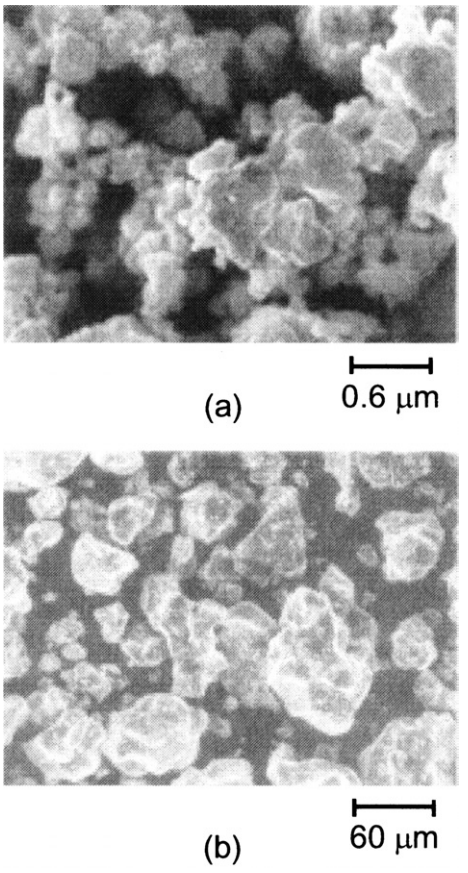

Fig. 6 Scanning electron microscope images of Ag_3VO_4 prepared (a) by precipitation and (b) by solid-state reactions. Acceleration voltage: 10 kV.

The higher degree of crystallization of the calcined sample decreased the number of grain boundaries. These serve as a recombination centers between photogenerated electrons and holes. Therefore, the decrease in the number of grain boundaries results in an increase in the photocatalytic activity. Although well-crystallized β-$AgVO_3$ and $Ag_4V_2O_7$ powders were also prepared by a solid-state reaction, their activities were negligible. On the other hand, all silver vanadates showed no activity for H_2 evolution from an aqueous methanol solution under visible light irradiation ($\lambda > 420$ nm) because the conduction band level composed of V 3d orbitals is more positive than the reduction potential of water to form H_2 (0 V *vs.* NHE). Ag_3VO_4 photocatalysts evolved no gases from pure water under visible light irradiation ($\lambda > 420$ nm) and the color hardly changed. These results indicated that Ag^+ ions in the Ag_3VO_4 crystal were stable and not photoreduced.

Fig. 7 shows dependence of O_2 evolution from an aqueous silver nitrate solution over an Ag_3VO_4 photocatalyst upon cut-off wavelength (using cut-off filters and measuring the diffuse reflectance spectrum of Ag_3VO_4). The horizontal axis indicates the cut-off wavelength in which transmittance is almost 0%. The onset of the action spectrum was in accord with the diffuse reflectance spectrum indicating that the O_2 evolution reaction over Ag_3VO_4 photocatalytically proceeded by band gap excitation.

Conclusions

(1) The band gap of α-$AgVO_3$ is 0.6 eV smaller than that of α-$NaVO_3$. An electronic structure study for α-$AgVO_3$ by the density functional method revealed that the Ag 4d and O 2p

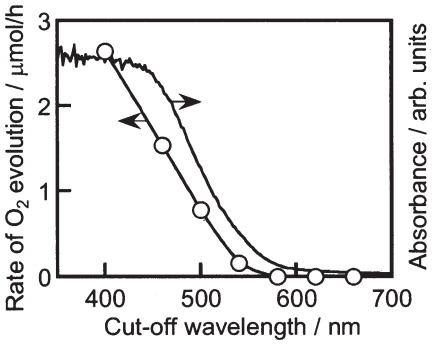

Fig. 7 Dependence of O_2 evolution from an aqueous silver nitrate solution over an Ag_3VO_4 photocatalyst upon cut-off wavelength (using filters and measuring the diffuse reflectance spectrum of Ag_3VO_4). Catalyst: 0.3 g, aqueous silver nitrate solution (0.05 mol L^{-1}, 150 mL), light source: 300 W Xe lamp, top irradiation cell.

orbitals formed the valence band at a more negative level than O 2p orbitals, resulting in the decrease in the band gap.

(2) Ag_3VO_4 showed photocatalytic activities for O_2 evolution from an aqueous silver nitrate solution under visible light irradiation. Thus, Ag_3VO_4 is a new visible-light-driven photocatalyst with an ability for O_2 formation.

(3) Ag_3VO_4 prepared by a solid-state reaction showed higher activity than that prepared by a precipitation reaction, because of the good crystallinity.

Acknowledgements

This work has been supported by Core Research for Evolutional Science and Technology (CREST) of Japan Science and Technology (JST) Corporation, a Grant-in-Aid (No.14050090) for the Priority Area Research (No.417) from the Ministry of Education, Culture, Science and Technology, and Tokyo Ohka foundation for the Promotion of Science and Technology.

References

1 A. Kudo, *J. Ceram. Soc. Jpn.*, 2001, **109**, S81.
2 K. Domen, J. N. Kondo, M. Hara and T. Takata, *Bull. Chem. Soc. Jpn.*, 2000, **73**, 1307.
3 A. Kudo, *Catal. Surv. Asia*, 2003, **7**, 31.
4 Z. Zou, J. Ye, K. Sayama and H. Arakawa, *Nature*, 2001, **414**, 625.
5 D. E. Scaife, *Solar Energy*, 1980, **25**, 41.
6 H. Kato and A. Kudo, *J. Phys. Chem. B*, 2002, **106**, 5029.
7 G. Hitoki, T. Takata, J. N. Kondo, M. Hara, H. Kobayashi and K. Domen, *Chem. Commun.*, 2002, 1698.
8 A. Kudo, K. Omori and H. Kato, *J. Am. Chem. Soc.*, 1999, **121**, 11 459.
9 H. Kato, H. Kobayashi and A. Kudo, *J. Phys. Chem. B*, 2002, **106**, 12 441.
10 K. Sayama, K. Mukasa, R. Abe, Y. Abe and H. Arakawa, *Chem. Commun.*, 2001, 2416.
11 S. Kittaka, K. Matsuno and H. Akashi, *J. Solid State Chem.*, 1999, **142**, 360.
12 F. Pascal, *Rev. Chim. Miner.*, 1969, **t. 6**, 819.
13 T. Hirono, H. Koizumi and T. Yamada, *Thin Solid Films*, 1987, **149**, L85.
14 M. C. Payne, M. P. Teter, D. C. Allan, T. A. Arias and J. D. Joannopoulos, *Rev. Mod. Phys.*, 1992, **64**, 1045.
15 H. Barker, *J. Chem. Soc. Dalton Trans.*, 1973, **15**, 1513.
16 P. Rozier, J. M. Savariault and J. Galy, *J. Solid State Chem.*, 1996, **122**, 303.